AIAA AVIATION Forum
12-16 June 2023, San Diego, CA and Online
AIAA AVIATION 2023 Forum

10.2514/6.2023-4389

Numerical Prediction of Generation of Axisymmetric Mode Jet Screech Tones at Different Mach Numbers

Rithik R. Nambiar*
Department of Aerospace Engineering, Indian Institute of Technology Bombay, Mumbai - 400072, INDIA

Karthik Sankar K.†
Department of Aeronautical and Automobile Engineering, Manipal Institute of Technology, Manipal Academy of Higher Education, Manipal - 576104, INDIA

Manikandan M.‡
Department of Aeronautical and Automobile Engineering, Manipal Institute of Technology, Manipal Academy of Higher Education, Manipal - 576104, INDIA

Manoj T. Nair§
Department of Aerospace Engineering, Indian Institute of Space Science and Technology, Thiruvananthapuram - 695547, INDIA

This paper presents a numerical prediction of the generation of axisymmetric mode jet screech tones, which are a significant contributor to jet noise in the aviation industry. The study uses a Pressure-based solver with a K-ϵ realization turbulence model to simulate the flow field and predict the frequency and amplitude of the tones. The simulations consider factors such as the nozzle geometry, exhaust gas velocity and temperature, and ambient conditions. The predictions are validated through experimental measurements, demonstrating the accuracy of the numerical methods. The screech tone frequencies and sound pressure levels in the near-field are in good agreement with the existing experimental data. The ability to numerically predict the generation of axisymmetric mode jet screech tones is an important tool for designing quieter aircraft engines, improving the comfort and safety of passengers and workers. From the simulated results, it is observed that the intensity of the screech tone is high at lower frequencies and higher Mach numbers.

I. Nomenclature

K	=	Turbulent Kinetic energy
ϵ	=	Kinetic energy dissipation
D	=	Nozzle exit diameter
λ	=	Acoustic wavelength
M	=	Mach number
γ	=	Specific heat ratio
P_t	=	Total gauge pressure

II. Introduction

Computational aeroacoustics (CAA) is a rapidly growing field that focuses on the simulation and prediction of noise generated by fluid flows. It combines computational fluid dynamics (CFD) techniques with acoustic theory to model the propagation of sound waves in the air and other fluids. CAA is used to study a wide range of noise sources,

*Project Research Assistant, Department of Aerospace Engineering, IIT Bombay, AIAA Non-Member
†M.Tech Student, Aeronautical and Automobile Engineering, MIT, Manipal, AIAA Non-member
‡Senior Assistant Professor, Aeronautical and Automobile Engineering, MIT, Manipal, AIAA Non-member
§Professor, Department of Aerospace Engineering, IIST, Thiruvananthapuram, AIAA Non-member

including jet engines, wind turbines, and automotive exhaust systems, and it plays a critical role in the design and optimization of these devices. With advances in high-performance computing and numerical methods, CAA has become an increasingly powerful tool for predicting and reducing noise in engineering applications.

Aeroacoustics plays a crucial role in aerospace vehicle design, certification, and performance. For commercial aircraft, engine noise has a significant impact on flight operations, including airport proximity and noise certification. In military aviation, aircraft noise poses health risks, including hearing loss, and creates communication challenges, especially in passenger planes. The sources of aircraft noise include exhaust jets, fans, and rotor blades. Acoustic noise is any intentional or unintentional sound in an acoustic environment, while noise in electronics may not be audible to the human ear and requires detection tools. Noise is defined as an unwanted sound that is loud, unpleasant, or disruptive. From a physical standpoint, there is no distinction between sound and noise, as both are vibrations of a medium like air or water. The difference arises in how the brain perceives and interprets sound.

The field of jet noise focuses on the turbulent eddies caused by shear flow and high-velocity jets in aeroacoustics. Jet noise consists of three levels of supersonic sound: turbulent mixing noise, broadband shock-associated noise, and screech tones. Screech tones are axisymmetric oscillations of the jet that are mainly illuminated upstream at low supersonic Mach numbers. Partially extended supersonic jets emit both broadband and frequency sound, including screech tones. Screech tones create a feedback loop driven by a high degree of unstable jet flow waves. The quasiperiodic shock cell structure within the jet plume generates instability interactions, waves, and shock cells, resulting in tone production.

Experimental data confirms that average speed profiles and the shock distribution of the shock cell jet are consistent with simulated values, including the frequency and intensity of screech tones and the direction of the jet-selected Mach numbers. Screech tones are produced by the feedback loop driven by waves of jet flow instability. The source of the partially extended jet is a structure of a quasiperiodic shock cell, and the acoustic pressure at the tip of the microphone, where the jet mixing layer is thinner, is pleasing. Waves of stable and unstable waves from a small flow multiply as they spread out on the ground. After spreading the range of four to five shock cells, a wave of instability interacts with quasiperiodic shock cells in the jet plume, producing acoustic radiation that spreads out of the jet. Acoustic waves delight the mixed layer of the jet when reaching the nozzle lip region, generating new waves of instability and closing the feedback loop.

This paper is focused on determining the jet shear layer in a steady state and transient state and also predicting the screech tones. These screech tones for the under-expanded supersonic jet are analyzed for different Mach numbers from different microphone locations at the nozzle lip.

III. Literature Review

In his research on supersonic jets, Tam [1] explains that turbulent jet flows typically contain both fine and large scales of turbulence, which together produce noise. However, the extent to which each type of turbulence contributes to sound production depends on factors such as the jet's Mach number and temperature, as well as the presence of sound-reflecting surfaces like impingement in the jet environment and the thickness of the nozzle lip. Tam goes on to describe the generation mechanism of screech tones, which results from an acoustic feedback phenomenon. This occurs when acoustic disturbances advance near the thin jet mixing layer close to the nozzle lip and external excitation is received, leading to the growth of instability waves as they propagate downstream. After four to five shock shells, a large enough amplitude is acquired, resulting in the generation of acoustic radiation primarily in the upstream direction in the case of Broadband shock-associated noise. This creates a feedback loop where the acoustic wave travels upstream outside the jet, generating new unstable waves and closing the loop as shown in Figure 1.

In their study, Hao Shen and Tam [2] showcased the potential of computational aeroacoustics methods in gaining insight into the physics and intricate mechanisms behind screech tone intensity and directivity. Their approach offers a reliable means of determining these phenomena, which differs from previous studies plagued by long-scale discrepancies and the need to address sound flow variations spanning multiple orders of magnitude. To overcome these issues, the researchers proposed a meticulous design of the computational grid and the use of high-order finite difference schemes, demonstrating their effectiveness in mitigating these problems.

Miller and Morris [3] conducted experimental works on Broad-Band Shock-associated noise, which is a dominant noise source in the upwards and side-line direction relative to the jet axis. The noise is characterized by multiple broadband peaks in the far field, caused by the meeting of jet shear layers and shock cell structures. To predict the noise components, the authors developed a BBSAN noise model using a two-equation turbulence model and applied it to rectangular and dual streams operating at high temperatures, off-design, and supersonic conditions. This model overcomes the limitations of previous models by relying solely on RANS CFD predictions and reducing the use of

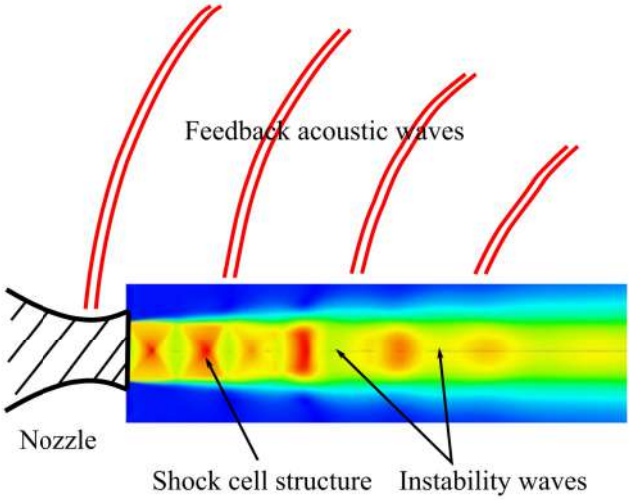

Fig. 1 Schematic diagram of the screech tone feedback loop (figure reproduced from [])

empiricism.

Kurbatskii et al. [4] utilized scale-resolving simulation to investigate the turbulent flow and acoustic field of a screeching supersonic jet. They discovered that using computational aeroacoustics methods for numerical simulation provides a novel way to comprehend the physics and detailed mechanisms of screech tone intensity and directivity. In another study, Kurbatskii et al. [5] conducted a numerical simulation of three-dimensional jet screech tones using a general-purpose finite-volume CFD code. They observed that careful grid design and the use of high-order finite difference schemes can address issues related to long-scale discrepancies and solve sound flow many orders of magnitude apart. Gojon et al. [6] examined the impact of impingement angle on the aeroacoustics feedback mechanism in supersonic planar jets. They found that sound-reflecting surfaces, such as impingements in the jet surroundings, have an impact on screech tone intensities.

Several studies have investigated the aerodynamics and aeroacoustics of supersonic jets and analyzed screech tones. Shen et al. [7] conducted numerical simulations to investigate axisymmetric mode jet screech tones and found that the screech frequency was related to the jet velocity and nozzle diameter. Sinibaldi et al. [8] studied impinging supersonic jets and found that the impinging distance and nozzle geometry significantly affected the screech frequency and intensity. Another study [9] focused on the flow field and noise characteristics of a supersonic impinging jet and found that the impinging distance, nozzle geometry, and Reynolds number played important roles in determining the noise characteristics. Spalart [10] proposed turbulence modelling and simulation methods for improving the accuracy of predictions for aeroacoustic phenomena. Norum [11] investigated screech suppression in supersonic jets using chevrons at the nozzle, which effectively modified the shock cell pattern and shear layer instability to suppress screech tones. Tam et al. [12] studied screech tones of supersonic jets from bevelled square nozzles and found that the bevel angle significantly affected the screech frequency. Hay et al. [13] investigated in-flight shock cell noise and found that the noise was directional and dependent on flight conditions. In a study on the mechanism of choked jet noise, Powell [14] discovered that the noise was produced by the interaction between shock cells and the turbulent mixing layer within the jet. The choking phenomenon had a significant impact on the noise characteristics. Similarly, Shen et al. [7] conducted a numerical simulation study to examine the generation of axisymmetric mode jet screech tones. Their findings indicated that the screech frequency was correlated with the jet speed and nozzle diameter, and the screech tones were mainly produced by the feedback mechanism between the shock cells and the shear layer in the jet.

IV. Methodology

The objective of this study is to identify the screech tone generated by a supersonic free-flow jet at Mach Numbers 1.2, 1.5, and 1.8 and to compare the results. The study involves analyzing an axisymmetric free jet that has a steady-state low supersonic flow. The analysis data is then calibrated to perform transient flow using the Realizable unsteady $k-\epsilon$ model. The output FFT plot data is then analyzed using spectral analysis to identify the screech tone. The simulation was conducted using *ANSYS*® 2022 R1, deployed in *ANSYS*® Fluent, and post-processing of the data was carried out in

CFD-Post.

A. Problem description

The aim of this research is to investigate the performance of an axisymmetric jet with different Mach numbers (1.2, 1.5, and 1.8) utilizing a round nozzle with a diameter of 1 inch and a wall-lip thickness of 0.625 inches. The study involves detecting the existence of screech tones by placing microphones at two distances (0.642 inches and 0.889 inches) along the wall lip. Notably, the simulation does not take into account the internal geometry of the nozzle, and the nozzle exit is considered as the inlet for the investigation.

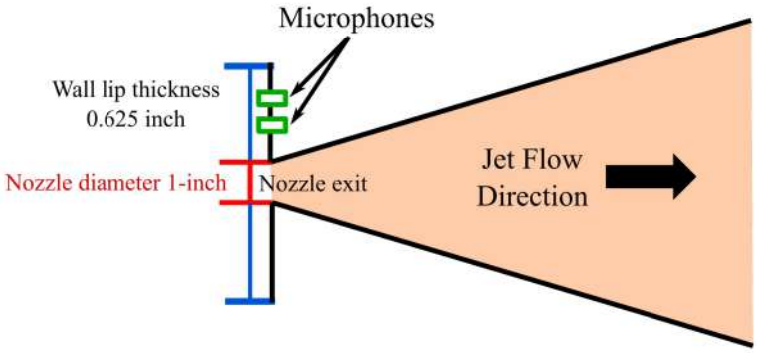

Fig. 2 Line diagram of the nozzle geometry

Figure 2 shows the line diagram of the geometry. The geometry dimensions and mesh parameters are furnished in Table 1. Two microphones are placed above the nozzle and along the wall lip. The coordinates of the microphones are given in Table 2.

Table 1 Geometry and mesh parameters

Parameters	Values
Round jet inlet diameter (inch)	1.000
Wall lip thickness (inch)	0.625
Far-field radius (inch)	1000
Nodes	1466904
Elements	1496645
Growth rate	1.2
Quadrilateral mesh size (m)	1e-4
Triangular mesh size (m)	1.5

Table 2 Microphone location coordinates

Microphone	x(m)	y(m)
Mic-1	0	0.0163
Mic-2	0	0.0226

B. Flow of work

The flowchart depicted in Figure 3 outlines the method utilized to examine the steady-state flow. This analysis is employed to establish the settings required to conduct the transient flow analysis, during which certain settings are modified. The transient analysis workflow is illustrated in Figure 4. These steps are applied to various Mach numbers.

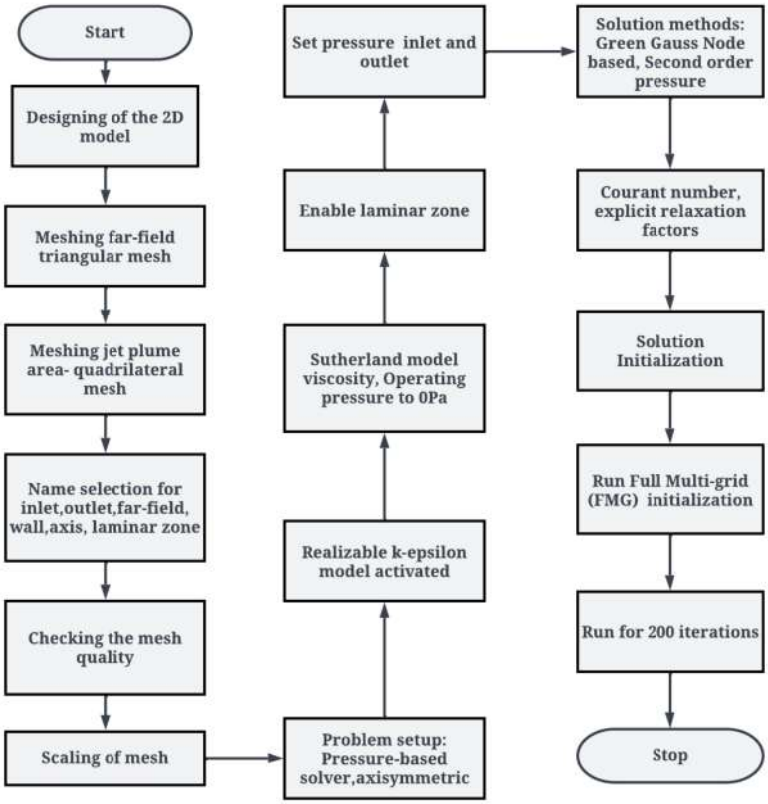

Fig. 3 Workflow of Steady-state Analysis

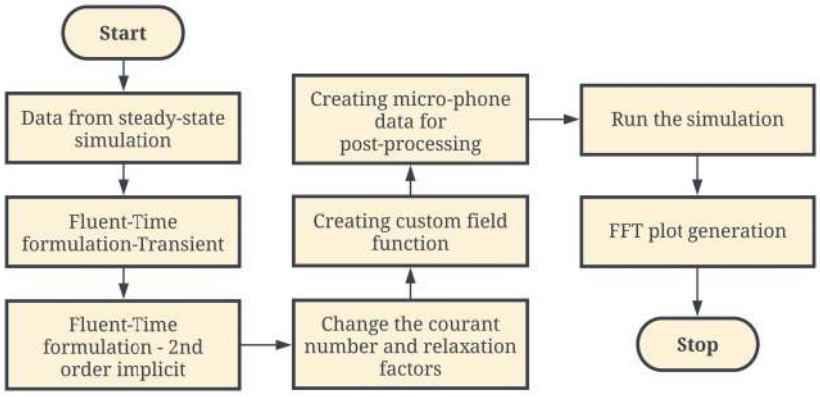

Fig. 4 Workflow of Transient-state Analysis

C. Mesh geometry

The meshing details for the simulation are illustrated in Figure 5. The far-field region is meshed with a triangular mesh with a sizing of 1.5m, while a quadrilateral mesh with a sizing of 0.0001m is employed for the turbulence region, jet plume, and laminar zone. Figure 6 depicts the mesh used, with an enlarged view of the turbulent zone. The simulation's small mesh size allows for precise resolution of the jet shear layer excitations at the nozzle tip, shear layer instability wave generation, shock cell structure formation in the nozzle core, and near-field propagation of screech acoustic waves.

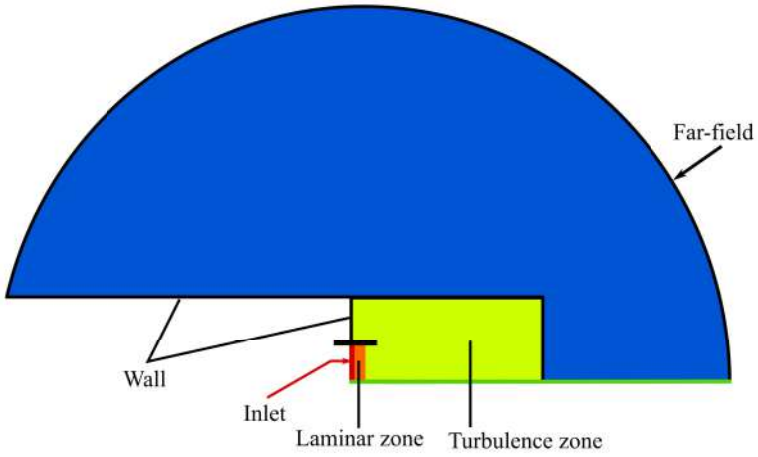

Fig. 5 Mesh domain

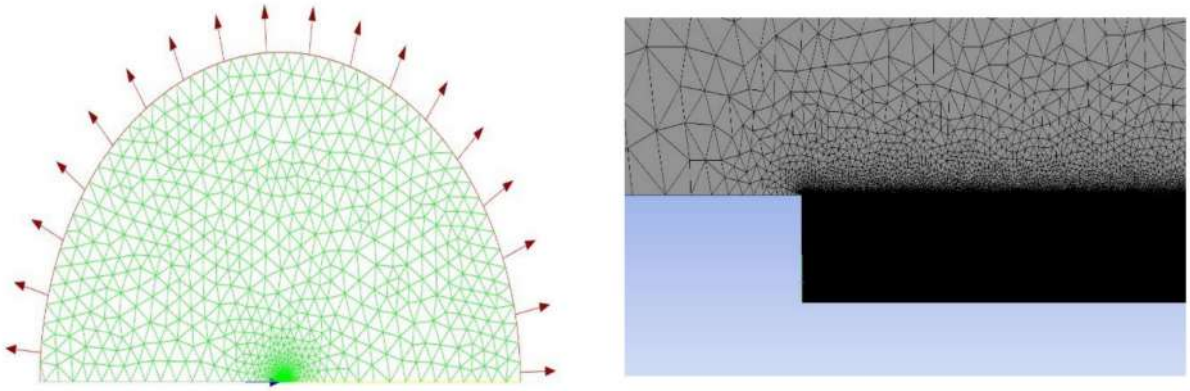

Fig. 6 Mesh display

D. Model setup

The initial phase of the model setup involves two steps. Firstly, checking the quality of the generated mesh to ensure accuracy and reliability, followed by scaling it to meters to obtain analysis results. To address the problem statement, a two-dimensional steady-state axisymmetric model is used, employing a pressure-based solver. The use of a structured mesh enables the higher-order QUICK discretization method in CFD, providing excellent resolution for parameters such as density, energy, and momentum, particularly when using a pressure-based solver.

To predict turbulent jet flows, the study employs the realizable k-ϵ viscous model with model constants adjusted by Tam and Thies [2]. This model is highly efficient and capable of delivering reliable results for complex problems. The Standard Wall Function is used for Near Wall Treatment. Table 3 presents the modified model constants.

Table 3 Realisable k-ϵ model constants

Model Constants	Values
C2-Epsilon	2.02
Turbulent Kinetic Energy Prandtl Number	0.324
Turbulent Dissipation rate Prandtl Number	0.377
Energy Prandtl Number	0.422

E. Cell zone and Boundary conditions

The current configuration utilizes compressed air in its optimal state as the working medium. Sutherland's Three Coefficient method is utilized to determine the fluid's viscosity, with the analysis presuming the density of an ideal gas. To enhance instability waves in the mixing layer, the nozzle is separated into two sections: a small laminar area and a larger turbulent area. This is done by setting the operating pressure to 0 Pa and assuming isentropic relations for the fully expanded jet operating at specific Mach numbers. At the nozzle exit, the turbulent intensity is considered low, with a value of 0.1. Furthermore, the jet is presumed to be cold, with a total temperature equal to the ambient static pressure.

Boundary Name	Type	Parameters
Inlet	Pressure inlet	▪ Initial Gauge Pressure: 127360 Pa ▪ Turbulence Intensity: 0.1% ▪ Hydraulic Diameter: 0.0254 m ▪ Temperature: 300 K
Far-field	Pressure outlet	▪ Gauge Pressure: 1e5 Pa ▪ Backflow Turbulence Intensity: 1% ▪ Backflow Turbulence Viscosity Ratio: 2 ▪ Backflow Temperature: 300 K
Wall	Wall	▪ Shear Condition: Specified Shear → X – component Shear: 0 Pa → Y – component Shear: 0 Pa ▪ Roughness Constant: 0.5 ▪ Heat Flux: 0 W/m^2

Fig. 7 Details of Boundary conditions

The slip walls are utilized in modeling the walls since the screech tones, generated by free jet flows, are minimally influenced by them. The boundary conditions data can be found in Figure 7. By configuring the simulation in this manner, the researchers can conduct a more thorough analysis of the screech tones generated by the jet flows. This data can then be employed to enhance the efficiency and optimize the design of supersonic jets. The aerospace industry regards the analysis of supersonic jet flows as crucial, as it is instrumental in the creation and advancement of various aircraft and spacecraft, such as military jets, supersonic transport aircraft, and rocket engines.

To calculate the Total Gauge pressure at various Mach numbers, a static pressure of $1e^5$ Pa was used, and the isentropic relation for pressure was applied to determine the stagnation pressure, as shown below.

$$\frac{P}{P_t} = \left(1 + \frac{\gamma - 1}{2} M^2\right)^{\frac{-\gamma}{\gamma - 1}} \tag{1}$$

From the above equation, total stagnation pressure is calculated. The calculated total stagnation pressure for given Mach numbers is given in Table 4.

Table 4 Gauge total pressure for corresponding mach number

Mach Number	P/P_t	Gauge total pressure (Pa)
1.2	0.4124	242496.5
1.5	0.2724	367107.2
1.8	0.1740	574712.6

F. Solution Methods, Controls and Initialization

The Pressure-Velocity coupling scheme is commonly utilized in solution methods due to its ability to provide a robust and efficient single-phase implementation for steady flows, resulting in optimal performance. However, the coupled algorithm becomes necessary for transient flows characterized by large time steps.

Regarding gradient evaluations, the Green-Gauss node-based scheme has been observed to outperform other methods. As mentioned earlier in this chapter, using QUICK discretization for density, momentum, and energy improves the performance of a pressure-based solver.

The Courant Number is a dimensionless value used in transient simulations to determine the appropriate time step for a given mesh size and flow velocity. In this particular test case, a Courant Number of 50 is set. The initialization data for the flow are provided in Table 5.

Table 5 Data for flow initialization

Initialization Parameter	Value
Gauge Pressure	100000 Pa
Axial Velocity	0 m/s
Radial Velocity	0 m/s
Turbulent Kinetic Energy	0.1 m^2/s^2
Turbulent Dissipation Rate	6 m^2/s^3
Temperature	300 K

G. Full Multi-Grid initialisation

FMG initialization is only applicable for steady-state problems. It offers an initial solution at the beginning of the calculation to accelerate flow convergence. By providing an approximate solution at minimal cost, FMG initialization outperforms complex computations that increase computational cost. The FMG initialization code is provided in the annexure for easy implementation.

H. Steady-state and Transient-state calculations

The steady-state analysis is performed for 200 iterations and the resulting data is post-processed using CFD-Post to obtain a steady-state shock structure and Mach number contour. In order to optimize the analysis, it is necessary to carefully examine the data results obtained from the steady-state analysis. For the transient analysis, the Time Formulation is modified to Transient and a Second-order Implicit Transient Formulation is introduced in the Solution Methods. To remove Implicit Relaxation factors from coupled equations, it is recommended to increase the value of the Courant number to $1e^{-15}$ for the transient pressure-based coupled solver. The Explicit and Under-Relaxation factors are set to 1. Table 6 lists the parameters required for iterating the transient flow. Post-processing of the simulation is carried out in CFD-Post after 20000 iterations.

Table 6 Transient flow iteration parameters

Parameters	Value
Time stepping method	Fixed
Time step size	5e-06
Number of time steps	2000
Max Iterations per time step	10

I. Acoustic post-processing

The Ffowcs-Williams and Hawkings Acoustic model has been integrated, and microphones have been placed at different locations along the jet's wall lip to enable FFT spectral analysis. The resulting spectral analysis plot employs Fast Fourier Transform, with frequency displayed on the x-axis and Sound Pressure Level (SPL) on the y-axis. To ensure that the plot is within the desired range, any values exceeding the range are clipped, enabling the contour to display within the pre-determined range.

Once the solver has been configured with these settings, the model is simulated, and the output is analyzed to comprehend the behavior of the generated screech tone. Based on the output data, the behavior is observed, analyzed, and conclusions are drawn.

V. Results and Discussions

A. Steady-state analysis

A steady-state analysis has been conducted to calibrate a model for simulating transient-state analysis in predicting the jet-shear layer. Velocity contours for Mach numbers of 1.2, 1.5, and 1.8 have been computed and depicted in Figures 8a,8b, and 8c, respectively. These figures show the formation of shock-cell structures starting from the nozzle exit in all three cases.

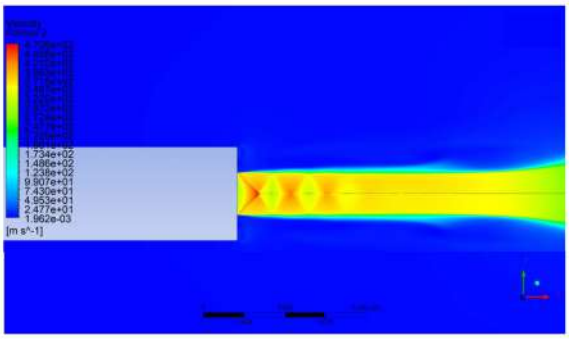

(a) At Mach number = 1.2

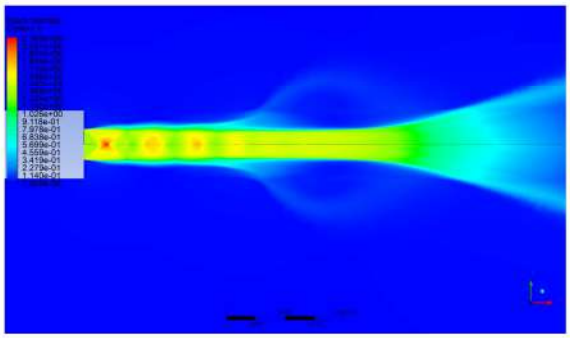

(b) At Mach number = 1.5

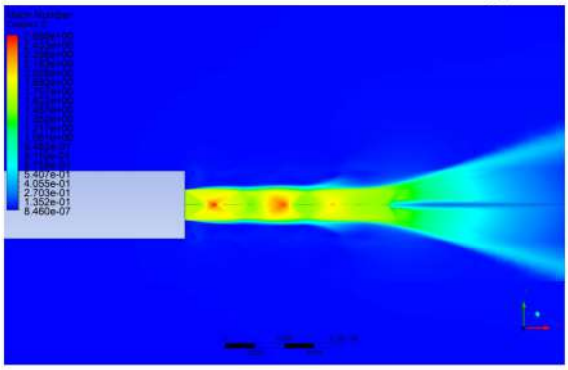

(c) At Mach number = 1.8

Fig. 8 Shock-cell formation in steady-state simulation

The figures depicted reveal that for a Mach number of 1.2, there are three to four shock cells formed, two to three shock cells for a Mach number of 1.5, and approximately two shock cells formed for Mach 1.8 before dissipation occurs. However, it should be noted that the number of shock cells formed may differ in each simulation due to the sensitivity of the jet screech mechanism, which is unique to the experimental setup. This emphasizes the significance of carefully controlled experimental conditions to study the phenomenon accurately [11].

B. Transient-state analysis

A discernible difference in the velocity contour can be observed between steady-state and transient-state simulations, where the shock-cell structure in steady-state is subdued. Transient simulations offer an efficient and more approximate solution than steady-state simulations. The formation of shock structures during transient state simulations is apparent.Figure 9a depicts the prominent formation of shock cells for Mach number 1.2, while the strength of the shock cells diminishes as the Mach number increases from 1.5 to 1.8, as demonstrated in Figures 9b and 9c respectively. Furthermore, it can be observed that the shock cell width is narrower for Mach 1.2 compared to higher Mach numbers.

C. Validation study

The validation process followed the methodology proposed by Kurbatskii [4]. Two microphones were placed at the nozzle lip to predict the behavior of the screech tone at Mach 1.2, with the screech peak frequencies serving as a crucial parameter for validation. Despite the simulation's sensitivity [11], the screech peaks remained stable, with insignificant

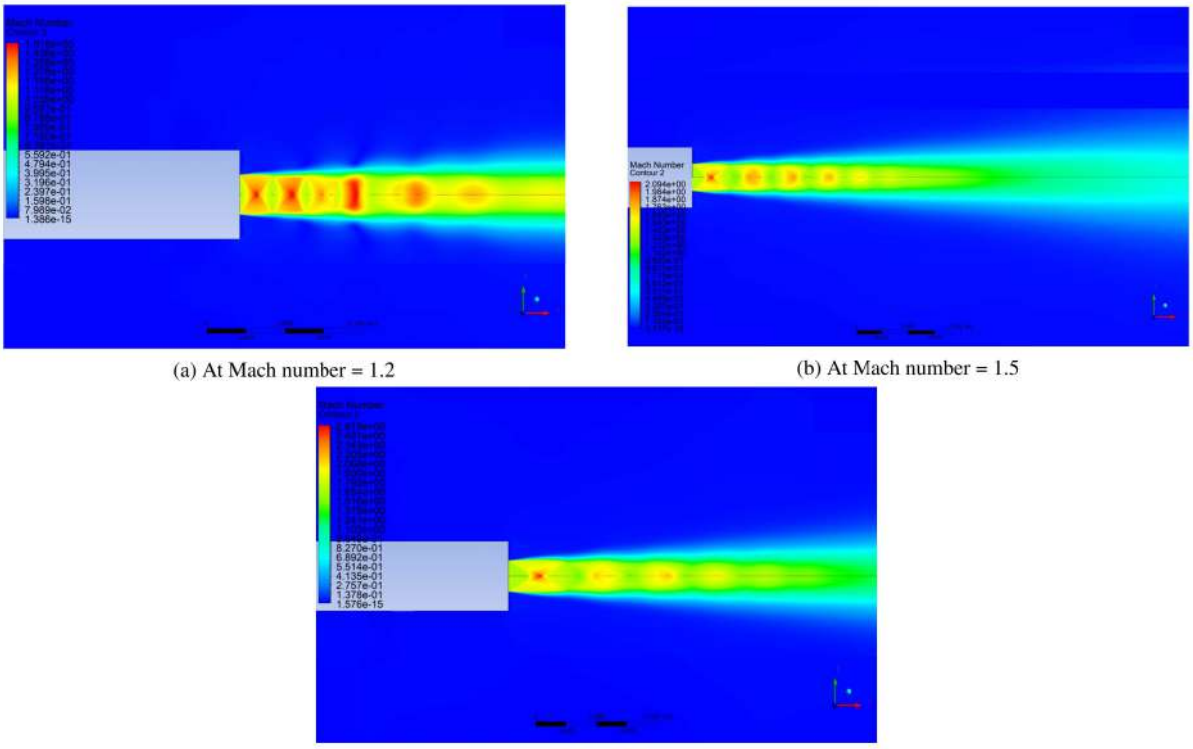

(a) At Mach number = 1.2

(b) At Mach number = 1.5

(c) At Mach number = 1.8

Fig. 9 Shock-cell formation in transient-state simulation

changes in their values as shown in Figure 10. However, the sound pressure levels were found to be susceptible to minor fluctuations due to mesh variations, turbulence constants, and other unpredictable environmental factors during numerical simulations. The screech tones were predominantly observed in the frequency range of $6-7$ kHz, with an average error of 1% detected during the validation process.

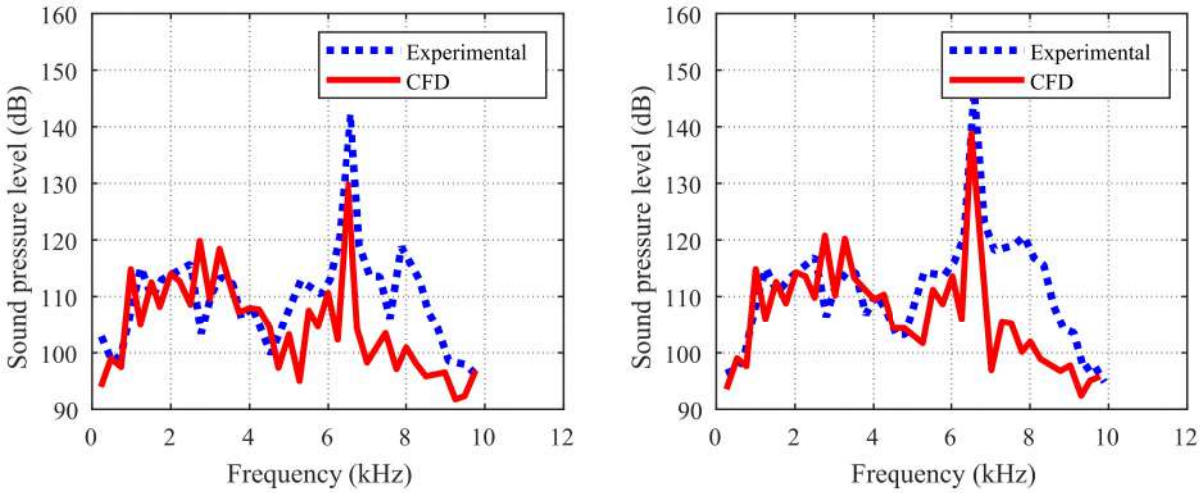

Fig. 10 Numerical validation of screech tones from Mic 1 and 2 at Mach 1.2 [4]

D. Sound pressure level analysis

The SPL vs Frequency graph displays screech tones detected at various Mach numbers. The FFT plots of Microphone 1 and Microphone 2 positioned on the nozzle lip reveal the presence of screech tone modes at each Mach number, as evidenced by the spikes observed in both plots. Notably, the highest sound pressure peak between 6000 – 7000 Hz is consistent with experimental data from Ponton and Seiner [15]. Additionally, analysis is shown in Figure 11 for M = 1.5 demonstrates a peak between 4000 – 5000 Hz, while Figure 12 shows a peak around 2000 Hz for M = 1.8. This observation suggests that, for an under expanded supersonic jet with a given inlet diameter, an increase in Mach number results in screech tone peaks occurring at lower frequencies

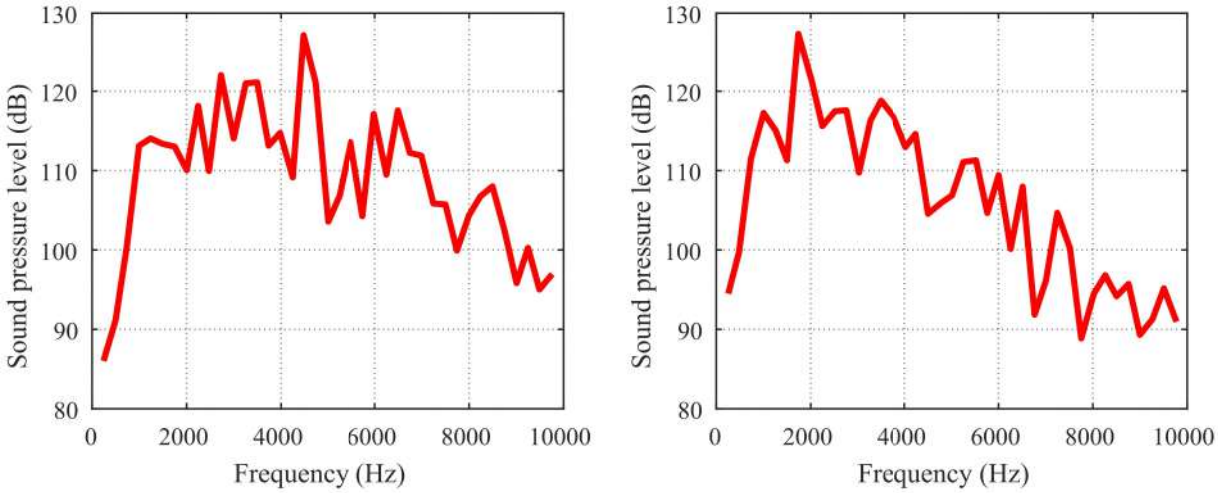

Fig. 11 Spectral plot for Mach 1.5 and 1.8 from Mic 1

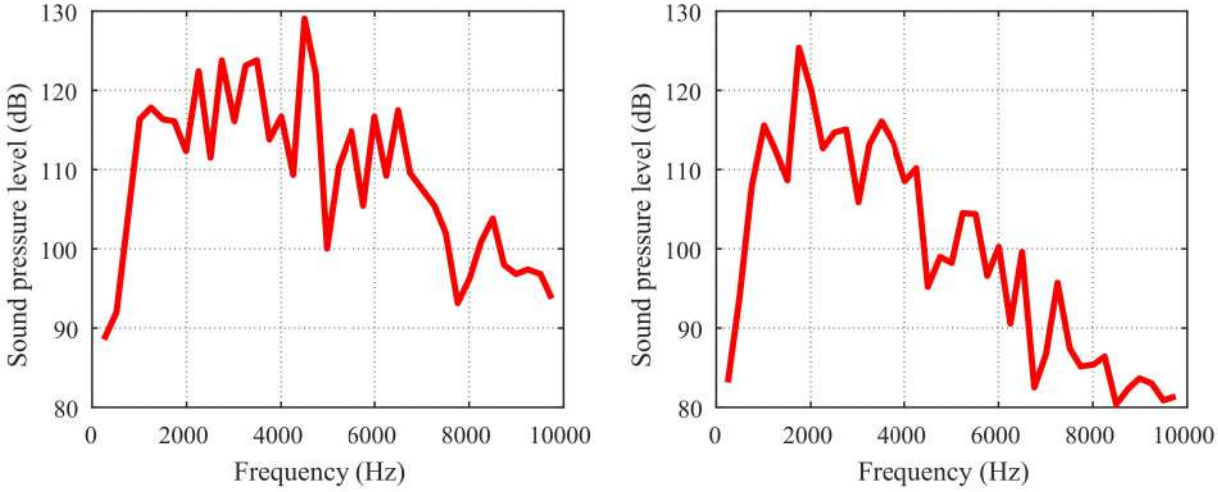

Fig. 12 Spectral plot for Mach 1.5 and 1.8 from Mic 2

VI. Conclusions

The main goal of this study is to enhance the accuracy of predicting jet screech noise generated from a supersonic jet nozzle exit at various Mach numbers using numerical simulation models in computational aeroacoustics. The lack of a mathematical formula to calculate the intensity and determine the direction of screech tone is addressed by improving prediction accuracy through an extensive investigation and comparison with experimental data.

To achieve this, a realizable k-ϵ viscous model was used due to its efficiency and accuracy in simulations. The steady-state analysis was employed to optimize the model, and the calibrated data was used to simulate the transient state with adjusted settings for improved accuracy. The results were further enhanced by introducing a pressure-based solver in the simulation. Following the transient simulation, microphone data was collected and post-processing was conducted.

The spectral analysis involved using FFT plots with sound pressure level on the y-axis and frequency on the x-axis. The results showed a spike in sound pressure level between the frequency range of 6000 Hz to 7000 Hz for M = 1.2, indicating the presence of screech tone in the free supersonic jet flow. Additionally, comparing the frequency at which jet screech peaks are seen revealed that an increase in Mach number leads to a decrease in the frequency at which the peak is obtained. Furthermore, Mach contours demonstrated that as Mach number increases, the strength of shock waves decreases, and the Mach cone width narrows.

References

[1] Tam, C. K., "Supersonic jet noise," *Annual review of fluid mechanics*, Vol. 27, No. 1, 1995, pp. 17–43.

[2] Tam, C., and Thies, A., "Computation of turbulent axisymmetric and nonaxisymmetric jet flows using the k model," *AIAA Journal*, Vol. 34, 1996, pp. 309–316.

[3] Miller, S., and Morris, P., "The prediction of broadband shock-associated noise from dualstream and rectangular jets using RANS CFD," *16th AIAA/CEAS Aeroacoustics Conference*, 2010, p. 3730.

[4] Kurbatskii, K., "Numerical simulation of three-dimensional jet screech tones using a general purpose finite-volume CFD code," *49th AIAA Aerospace Sciences Meeting including the New Horizons Forum and Aerospace Exposition*, 2011, p. 1085.

[5] Kurbatskii, K., "Scale-resolving simulation of an unsteady turbulent flow and acoustic field of a screeching supersonic jet," *18th AIAA/CEAS Aeroacoustics Conference (33rd AIAA Aeroacoustics Conference)*, 2012, p. 2289.

[6] Gojon, R., and Bogey, C., "Effects of the angle of impact on the aeroacoustic feedback mechanism in supersonic impinging planar jets," *International Journal of Aeroacoustics*, Vol. 18, No. 2-3, 2019, pp. 258–278.

[7] Shen, H., and Tam, C. K., "Numerical simulation of the generation of axisymmetric mode jet screech tones," *AIAA journal*, Vol. 36, No. 10, 1998, pp. 1801–1807.

[8] Sinibaldi, G., Lacagnina, G., Marino, L., and Romano, G. P., "Aeroacoustics and aerodynamics of impinging supersonic jets: Analysis of the screech tones," *Physics of Fluids*, Vol. 25, No. 8, 2013, p. 086104.

[9] Krothapalli, A., Rajkuperan, E., Alvi, F., and Lourenco, L., "Flow field and noise characteristics of a supersonic impinging jet," *Journal of Fluid Mechanics*, Vol. 392, 1999, pp. 155–181.

[10] Spalart, P. R., "Strategies for turbulence modelling and simulations," *International journal of heat and fluid flow*, Vol. 21, No. 3, 2000, pp. 252–263.

[11] Norum, T., "Screech suppression in supersonic jets," *Aiaa Journal*, Vol. 21, No. 2, 1983, pp. 235–240.

[12] Tam, C. K., Shen, H., and Raman, G., "Screech tones of supersonic jets from bevelled rectangular nozzles," *AIAA journal*, Vol. 35, No. 7, 1997, pp. 1119–1125.

[13] Hay, J., and Rose, E., "In-flight shock cell noise," *Journal of Sound Vibration*, Vol. 11, No. 4, 1970, pp. 411–IN3.

[14] Powell, A., "On the mechanism of choked jet noise," *Proceedings of the Physical Society. Section B*, Vol. 66, No. 12, 1953, p. 1039.

[15] Ponton, M., and Seiner, J., "The effects of nozzle exit lip thickness on plume resonance," *Journal of Sound and Vibration*, Vol. 154, No. 3, 1992, pp. 531–549.